

# Spectropolarimetric diagnostics of thermonuclear supernova explosions

Lifan Wang<sup>1,2</sup> \*, Dietrich Baade,<sup>3</sup> Ferdinando Patat<sup>3</sup>

<sup>1</sup>Physics Department, Texas A&M University, College Station, Texas, 77843-4242

<sup>2</sup>Lawrence Berkeley National Laboratory, 1 Cyclotron Rd, Berkeley, CA 94710

<sup>3</sup>European Southern Observatory, Karl-Schwarzschild-Strasse 2, D-85748 Garching, Germany

**Even at extragalactic distances, the shape of supernova ejecta can be effectively diagnosed by spectropolarimetry. We present here results for 17 Type Ia supernovae that allow a statistical study of the correlation among the geometric structures and other observable parameters of Type Ia supernovae. These observations suggest that their ejecta typically consist of a smooth, central iron rich core and an outer layer with chemical asymmetries. The degree of this peripheral asphericity is correlated with the light-curve decline rate of Type Ia supernovae. These observations lend strong support to delayed-detonation models of Type Ia supernovae.**

Different supernova explosion mechanism may lead to differently structured ejecta. Type

---

\*To Whom correspondence should be addressed. E-mail: wang@physics.tamu.edu

Ia supernovae (SNe) have been used as a premier tool for precision cosmology. They occur when a carbon/oxygen white dwarf reaches the Chandrasekhar stability limit, probably due to mass accretion in a binary system, and is disrupted in a thermonuclear explosion (1). It is, however, a matter of decade-long debate how the explosive nuclear burning is triggered and how it propagates through the progenitor star (2, 3, 4, 5, 6). Successful models generally start with a phase of sub-sonic nuclear burning, or deflagration, but theorists disagree on whether the burning front becomes supersonic following the earlier phase of deflagration. An explosion that does turn into supersonic burning is called delayed-detonation (4). The resulting chemical structures are dramatically different for deflagration (5) and delayed-detonation models (7). For a pure deflagration model, chemical clumps are expected to be present at all velocity layers that burning has reached (5). For delayed-detonation, the detonation front propagates through the ashes left behind by deflagration and burns partially burned or unburned elements further into heavier elements, and erases the chemically clumpy structures generated by deflagration.

The polarized emission from a supernova is caused by electron scattering in its ejecta. It is sensitive to the geometric structure of the ejecta (8). Electron scattering in an asymmetric ejecta would produce non-zero degrees of polarization (8). In continuum light, normal SNe Ia are only polarized up to about 0.3%, but polarization as high as 2% is found across some spectral lines (10, 11, 12, 13, 14, 15). The polarization decreases with time and vanishes around 2 weeks past optical maximum. The low level of continuum polarization implies that the SN Ia photospheres are, in general, approximately spherical. The decrease of polarization at later times suggests that the outmost zones of the ejecta are more aspherical than the inner zones. Similarly, the large polarization across certain spectral lines implies that the layers above the photosphere are highly aspheric and most likely chemically clumpy (13, 14, 16, 15).

In this study, we report polarimetry of 17 SNe Ia. These are all the SNe Ia for which we have pre-maximum polarimetry. The observations (Table 1) were collected with the 2.1-m Otto

Struve Telescope of the McDonald Observatory of the University of Texas and with one of the 8.2-m unit telescopes of Very Large Telescope (VLT) of the European Southern Observatory (ESO). The typical spectral resolution of these observations is 1.2 nm and the wavelength range is typically from 400nm to 850nm. The total exposure time is longer than 4 hours for the data taken with the 2.1-m telescope, and is around 1-2 hours for the ESO-VLT. Only SNe observed before optical maximum are included. We restrict ourselves to the characteristic Si II 635.5 nm line. More information about data acquisition and reduction is given in the Supporting Online Material.

The observed Stokes parameters can be projected onto the so-called principle and secondary axes, which are defined (9, 13) by a principle-component analysis of the data points on the Q-U diagram such that the spectral variation of the polarization is maximal along the principle axis. The secondary axis is orthogonal to the principal axis. As an example, in the spectra and principle components of the polarization of SN 2002bo at different epochs (Fig. 1), the polarized spectral features at 470.0 nm, and at 600.0 nm decreased significantly by day +14. The polarization data for SN 1996X, SN 1999by, SN 2001el, and SN 2004dt have been discussed in previous studies (11, 12, 13, 16, 14, 15) revealing a considerable level of individuality.

As a luminosity indicator we use the decline in  $B$  magnitude within 15 days from maximum ( $\Delta m_{15}$ ). This quantity is found to be well correlated with the intrinsic luminosity of SNe Ia (17): intrinsically dimmer SNe Ia usually show a faster decline, i.e. larger  $\Delta m_{15}$ . For those SNe with no published light curves, the luminosity indicator was derived from cross correlations of the flux spectra with a library of well-observed SNe Ia, and the  $\Delta m_{15}$  values of the closest spectral matches were adopted. The best matches to SN 2002fk, SN 2003W, SN 2004ef, SN 2005de, and SN 2005df are SN 1996X, SN 2002bo, SN 2001el, SN 2001el, and SN 1994D, respectively. The results are cross-checked with the ratio of the Si II absorption lines at 615 and 580 nm (18), and the results are generally in good agreement. For the SNe with no published light curves,

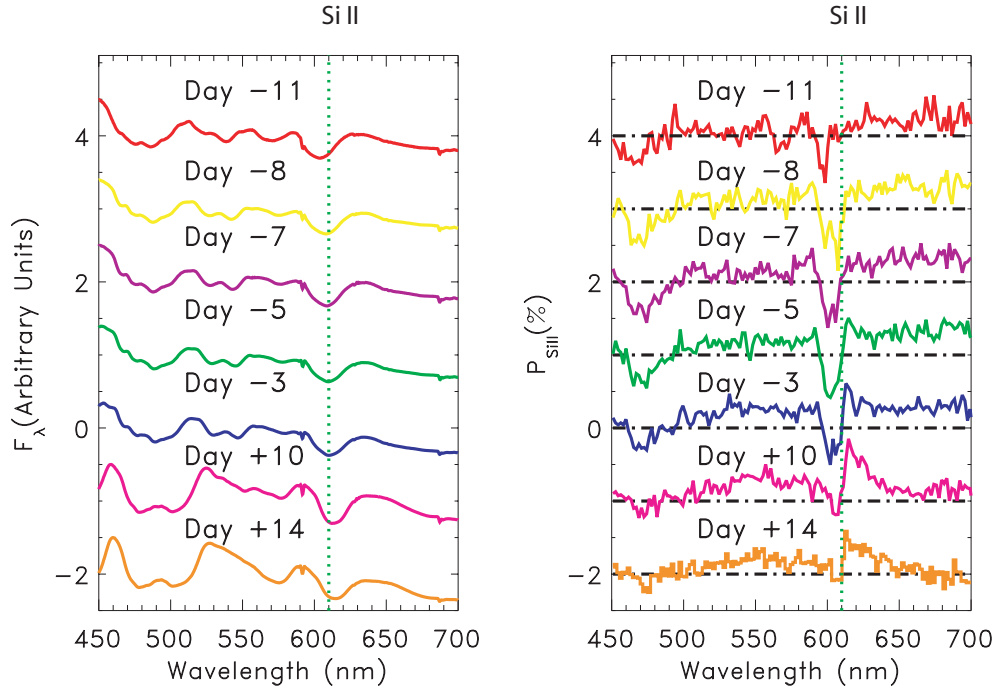


Figure 1: Spectroscopy (left) and spectropolarimetry (right) of SN 2002bo. The units of the fluxes on the left panel are arbitrary, from top to bottom, the zero point of each spectrum is offset from zero by 4, 3, 2, 1, 0, -1, and -2 for clarity. On the right hand side panel, from top to bottom, the degree of polarization of each observation is offset by 4%, 3%, 2%, 1%, 0%, -1%, and -2%. In both panels, the vertical dotted line mark the absorption features of the Si II lines.

0.05 mag is quadratically added to the errors of  $\Delta m_{15}$  deduced from the light curve of the best matching spectral template. All  $\Delta m_{15}$  values derived from published light curves are based on our light-curve fitting procedure (19).

The degree of polarization is known to evolve with time. To compare the data at the same epoch, the time dependence of the polarization of all the Branch normal SNe is fitted by a second order polynomial (shown in Figure S1) and the polarization data are then corrected to 5 days before peak  $B$  magnitude. Excluding peculiar events SN 2001V, SN 2004dt, and SN 1999by, (see Supporting Online Material), the correlation is fitted by a linear relation

$P_{SiII} = 0.48(03) + 1.33(15)(\Delta m_{15} - 1.1)$ . The Pearson correlation coefficient is 0.87 which suggests a strong correlation. The  $\chi^2$  of the linear fit is 16 with 13 degrees of freedom.

As the continuum polarization is generally low ( $\sim 0.2$ ) for SN Ia, the ejecta is likely to be chemically clumpy to explain the observed high polarization across spectral lines (14). If this is the case, projection effects must play a role in diluting this correlation (Fig. 2). This might be the case for the significant deviation of SN 2004dt from the regression line (Fig. 2). When viewed in certain directions, the degree of polarization can be particularly large or small. A tight correlation could only be expected for the mean degree of polarization averaged over several SNe and at the same photometric phase. To quantify this effect, we have constructed a toy-model which assumed that the disk of the supernova photosphere is polarized at 11.73% (20) at the limb, and decreases quadratically with distance from the limb to the center to zero polarization (see also the Supporting Online Material). We performed a Monte-Carlo simulation which assumes  $N$  opaque clumps, each covering an area  $S$  along the line of sight to the photosphere. The depth of the P-Cygni absorption feature (defined as the ratio of flux at the minimum of the absorption feature to that of the continuum) is then  $1 - NS/\pi R^2$ , where  $R$  is the radius of the photosphere. For lines about 50% deep ( $NS/\pi R^2 = 0.5$ ), the probability distribution of the polarization is found to peak at around 0.5% for  $N = 20$ . The  $1 - \sigma$  width of this distribution calculated assuming  $NS/\pi R^2 = 0.5$  (Fig. 2) envelopes most of the observed data points. In reality, there is a wide range of Si II line strengths, accordingly the numbers and sizes of lumps may not be the same for all the SNe. The observed polarization- $\Delta m_{15}$  correlation appears to be tighter than given by the Monte-Carlo model. This is perhaps an indication of a non-negligible amount of large scale asymmetry of the SN ejecta, especially for those SNe with high polarization and  $\Delta m_{15}$ . Such large scale asymmetries do not generate noticeable amounts of polarization in the continuum, which is formed deeper inside, and can be due to large plumes located above the SN photosphere. It may also be generated from the interaction of the ejecta

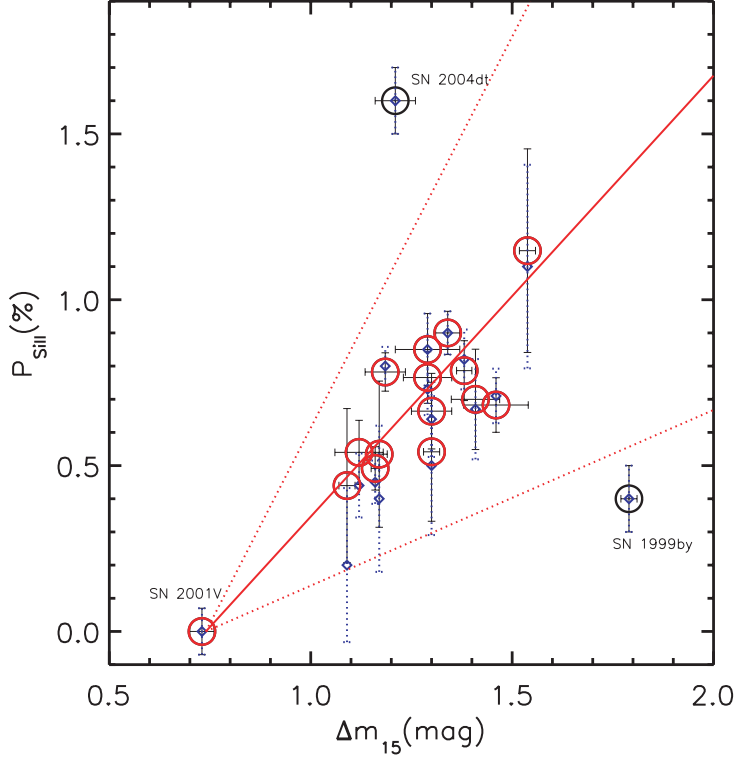


Figure 2: The correlation between the degree of polarization across the Si II 635.5 nm line and the light curve decline rate  $\Delta m_{15}$  for a sample of 17 Type-Ia SNe. The blue diamonds are the measured values as given in Table 1. The open circles show the data corrected to day -5, by subtracting  $0.041(t + 5) + 0.013(t + 5)^2$  from the observed degree of polarization, where  $t$  is the day after optical maximum. This correction formula was derived from a weighted quadratic fit to the time dependence of polarization (shown in the insert). The linear fit represented by the straight line includes only spectroscopically normal SNe shown as red open circles. The blue open circle shows the highly polarized event SN 2004dt, and the sub-luminous SN 1999by. The dotted-lines illustrate the  $1\text{-}\sigma$  level of the intrinsic polarization distribution around the most-likely value for the Monte-Carlo simulation described in the text.

with the circumstellar material such as an accretion disk before the explosion of the white dwarf progenitor. Alternatively, the observed tight correlation may also be due to a global aspherical explosion. In this case, a tight correlation implies more asymmetric explosion generates intrinsically dimmer SNe. However, we stress that the asymmetries we observed here are confined to the high velocity regions and do not affect the geometric shape of SN photosphere around optical maximum. Any large scale asymmetry is therefore confined only to the outmost layers.

As the light curve of SN Ia is powered by the radioactive decay of  $^{56}\text{Ni}$ , we infer (Fig. 2) a possible anti-correlation between the amount of  $^{56}\text{Ni}$  synthesized in SNe Ia and the asphericity of the silicon rich layer.

Our discovery puts strong constraints on any successful models of SNe Ia. At around optical maximum, the photosphere is typically located at velocities around 12,000 km/sec as measured from P-cygni line profiles, which according to hydrodynamic calculations (7) of delayed-detonation, is close to the velocity zones dominated by iron group elements. The absence of significant polarization at this velocity is evidence in support of delayed-detonation.

Details of delayed-detonation models affect the brightness of SNe Ia and their geometric structure. Larger departures from sphericity imply less of the central region is scoured of irregularities in the composition left by pure deflagration models, and thus less material burned to thermonuclear equilibrium and hence dimmer SNe, in accordance with the statistical trend revealed by our studies.

Finally, we make some remarks on using SNe Ia as standard candles. Asymmetry introduces intrinsic magnitude and color dispersions. Intrinsic color dispersion may be particularly important as it makes it difficult to perform precise extinction corrections. The stochastic nature of the origin of the asymmetry suggest that the color corrections can only be performed in a statistical sense. It is perhaps difficult to find pairs of SNe Ia with identical light-curve and spectroscopic properties.

In summary, the application of spectropolarimetric observing techniques to SNe Ia permits the geometric structures of SNe to be probed even though they are at distances that cannot be spatially resolved. The explosion of SNe Ia is intrinsically a 3-D phenomenon, and a phase of delayed detonation is necessary to account for the observed geometric and chemical differentiation.

## References and Notes

1. Whelan, J. & Iben, I. J. Binaries and Supernovae of Type I. *Astroph. J.* **186**, 1007-1014 (1973)
2. Arnett, D. A Possible Model of Supernovae: Detonation of  $^{12}\text{C}$ . *Astrophys. Space Sci.*, **5**, 180-212 (1969)
3. Nomoto, K., Sugimoto, D., & Neo, S. Carbon Deflagration Supernova, An Alternative to Carbon Detonation. *Astrophys. & Space Sci.*, **39**, L37-L42 (1976)
4. Khokhlov, A. M. Delayed Detonation Model for Type Ia Supernovae. *Astron. Astroph.* **245**, 114-128 (1991)
5. Reinecke, M., Hillebrandt, W., & Niemeyer, J. C. Three-dimensional Simulations of Type Ia Supernovae. *Astron. Astroph.* **391**, 1167-1172 (2002)
6. Plewa, T., Calder, A. C., Lamb, D. Q. Type Ia Supernova Explosions: Gravitationally Confined Detonations. *Astroph. J.*, **12**, L37-L40 (2004)
7. Gamezo, V. N., Khokhlov, Alexei M., Oran, Elaine S. Three-dimensional Delayed-Detonation Model of Type Ia Supernovae. *Astroph. J.* **627**, 337-346 (2005)



8. Höflich P. Asphericity Effects in Scattering Dominated Photospheres. *Astron. Astroph.* **246**, 481-489 (1991)
9. Wang, L., Howell, D. A., Höflich, P., & Wheeler, J. C. Bipolar Supernova Explosions. *Astroph. J.* **550**, 1030-1035 (2001)
10. Wang, L., Wheeler, J. C., Li, Z., & Clocchiatti, A. Broadband Polarimetry of Supernovae: SN 1994D, SN 1994Y, SN 1994ae, SN 1995D, and SN 1995H. *Astroph. J.* **467**, 435-445 (1996)
11. Wang, L., Wheeler, J. C., & Höflich, P. Polarimetry of the Type Ia Supernova SN 1996X. *Astroph. J.* **476**, L27-L30 (1997)
12. Howell, D. A., Höflich, P., Wang, L., & Wheeler, J. C. Evidence for Asphericity in a Subluminous Type Ia Supernova: Spectropolarimetry of SN 1999by. *Astroph. J.* **556**, 302-321 (2001)
13. Wang, L. *et al.* Spectropolarimetry of SN 2001el in NGC 1448: Asphericity of a Normal Type Ia Supernova. *Astroph. J.* **591**, 1110-1128 (2003)
14. Wang, L. *et al.* Pre-Maximum Spectropolarimetry of the Type Ia SN 2004dt. *Astroph. J.* in press, astro-ph/0409593 (2006)
15. Leonard, D. C., *et al.* Evidence for Spectropolarimetric Diversity in Type Ia Supernovae. *Astroph. J.*, **632**, 450-475 (2005)
16. Kasen, D. *et al.* Analysis of the Flux and Polarization Spectra of the Type Ia Supernova SN 2001el: Exploring the Geometry of the High-Velocity Ejecta. *Astroph. J.* **593**, 788-808 (2003)
17. Phillips, M. M. The absolute magnitudes of Type IA supernovae. *Astroph. J.* **413**, L105-L108 (1993)

18. Nugent, P. E., Phillips, M. M., Baron, E., Branch, D., Hauschildt, P. H. Evidence for a Spectroscopic Sequence Among Type Ia Supernovae. *Astroph. J.*, 455, L147-L150 (1995)
19. Wang, L, Strovink, M. Conley, A., Goldhaber, G., Kowalski, M., Perlmutter, S., & Siegrist, J. Nonlinear Decline-Rate Dependence and Intrinsic Variation of Type Ia Supernova Luminosities. *Astroph. J.* **641**, 50-69 (2006)
20. Chandrasekha, S. Radiative Transfer, Dover, New York, p.22 (1960)
21. Riess, A. G. *et al.* BVRI Light Curves for 22 Type IA Supernovae. *Astron. J.* **117**, 707-724 (1999)
22. Jha, S. *et al.* UBVRI Light Curves of 44 Type Ia Supernovae. *Astroph. J.*, 131, 527-554 (2006)
23. Altavilla, G. *et al.* Cepheid Calibration of Type Ia Supernovae and the Hubble Constant. *Mon. Not. Royal Astron. Soc.* 349, 1344-1352 (2004)
24. Li, W. *et al.* The Type IA Supernova 1997BR in ESO 576-G40. *Astron. J.* **117**, 2709-2724 (1999)
25. Garnavich, P. M. *et al.* The Luminosity of SN 1999by in NGC 2841 and the Nature of “Peculiar” Type Ia Supernovae. *Astroph. J.* **613**, 1120-1132 (2004)
26. Vinkó, J. *et al.* The Type Ia Supernova 2001V in NGC 3987. *Astron. Astroph.* **397**, 115-120 (2003)
27. Krisciunas, K. *et al.* Optical and Infrared Photometry of the Nearby Type Ia Supernova 2001el. *Astron. J.* **125**, 166-180 (2003)

28. Benetti, S. *et al.* Supernova 2002bo: Inadequacy of the Single Parameter Description. *Mon. Not. Royal Astron. Soc.* **348**, 261-278 (2004)
29. Pastorello et al., private communication (2006)
30. We are grateful to the European Southern Observatory for the generous allocation of observing time. We especially thank the staff of the Paranal Observatory for their competent and never-tiring support of this project in service mode. The research of LW is supported in part by the Director, Office of Science, Office of High Energy and Nuclear Physics, of the U.S. Department of Energy under Contract No. DE-AC03-76SF000098. We are grateful to discussions with J. Craig Wheeler. The SN polarimetry project, on which this study is based, has greatly benefited from contributions by him and Peter Höflich. We are also grateful to the anonymous referees that helped to improve this paper. This work is based in part on observations obtained at the European Southern Observatory, Chile (Program IDs: 64.H-0617(B), 66.D-0328(A), 67.D-0517(A), 68.D-0571(A), 69.D-0438(A), 70.D-0111(A), 71.D-0141(A), 073.D-0771(A), and 075.D-0628(A))

Table 1: The identification, observing date, phase (in days relative to optical maximum light), telescope, intrinsic degree of polarization across the Si II 635.5 nm line,  $\Delta m_{15}$ , and references for  $\Delta m_{15}$  values

SN	Date of Obs	Phase	Telescope	$P_{SiII}$	$\Delta m_{15}$	References
1996X	1996/04/14	-4.2	McD 2.1 m	0.50(20)	1.30(02)	(21, 19)
1997bp	1997/04/07	-5.0	McD 2.7 m	0.90(10)	1.29(08)	(22, 19)
1997bq	1997/04/25	-3.0	McD 2.1 m	0.40(20)	1.17(02)	(22, 19)
1997br	1997/04/20	-2.0	McD 2.1 m	0.20(20)	1.09(02)	(24, 19)
1999by	1999/05/09	-2.5	McD 2.1 m	0.40(10)	1.79(01)	(25)
2001V	2001/02/25	-7.3	VLT	0.00(07)	0.73(03)	(26, 19)
2001el	2001/09/26	-4.2	VLT	0.45(02)	1.16(01)	(27, 19)
2002bo	2002/03/18	-5.0	VLT	0.90(05)	1.34(03)	(28, 19)
2002el	2002/08/14	-6.4	VLT	0.72(09)	1.38(05)	(19)
2002fk	2002/10/06	-5.5	VLT	0.67(10)	1.19(05)	see text
2003W	2003/01/31	-4.5	VLT	0.64(10)	1.30(05)	see text
2004dt	2004/08/13	-7.3	VLT	1.60(10)	1.21(05)	(29)
2004ef	2004/09/11	-4.1	VLT	1.10(30)	1.54(07)	see text
2004eo	2004/09/20	-5.9	VLT	0.71(08)	1.46(08)	(29)
2005cf	2005/06/01	-9.9	VLT	0.44(05)	1.12(06)	(29)
2005de	2005/08/06	-4.4	VLT	0.67(14)	1.41(06)	see text
2005df	2005/08/08	-4.3	VLT	0.73(05)	1.29(09)	see text